Photochemistry and Photobiology, 2018, 94: 343–350

Long-term Genoprotection Effect of *Sechium edule* Fruit Extract Against UVA Irradiation in Keratinocytes

Elodie Metral[1,2,3], Walid Rachidi[2], Odile Damour[3], Frédéric Demarne[1] and Nicolas Bechetoille[1]*

[1]R&D Department, Gattefossé, Saint-Priest, France
[2]CEA/INAC/SyMMES/CIBEST, University of Grenoble Alpes, Grenoble, France
[3]BTC/LSC HCL de Lyon, Lyon, France

Received 29 May 2017, accepted 5 October 2017, DOI: 10.1111/php.12854

ABSTRACT

Photoprotection is essential to prevent the long-term deleterious effects of ultraviolet (UV), including skin cancer and photoaging. So far, there has been an increase in the use of natural bioactive phytochemicals for the development of more effective skin photoprotective agents. However, the molecular mechanisms underlying the photochemoprotection activity of such compounds remain largely unknown. The objective of this study was to investigate the effects of a *Sechium edule* fruit extract (SEE) in terms of photoprotection against UVA in primary human keratinocytes. We found that SEE protected keratinocytes against UVA-induced cytotoxicity, decreased the intracellular amounts of reactive oxygen species, and reduced oxidatively induced DNA lesions after UVA exposure. Furthermore, SEE decreased the induction of CPD lesions in UVA-irradiated keratinocytes and exhibited increased DNA repair of such photoproducts at 24 h postexposure. Finally, using DNA repair biochips, we demonstrated that SEE-treated keratinocytes had DNA enzymatic repair activities more efficient for abasic sites, CPD and thymine glycols. Therefore, the benefits of SEE against UVA could be explained by a combination of antioxidant activity, the reduction in DNA damage, and the enhancement of DNA repair capacities.

INTRODUCTION

Epidermis is in a constant renewal to maintain its integrity and regeneration after wounding. It is the most responsive tissue to sun radiation which may lead to disruption of skin homeostasis. This explains why a growing interest is focused on the increased ultraviolet (UV) irradiation at the Earth's surface and its adverse effects on the skin. Specifically, DNA is one of the main targets for UV-induced damage in living cells. UV induces the formation of several types of mutagenic DNA lesions according to its wavelength components, including UVC (100–280 nm), UVB (280–315 nm), and UVA (315–400 nm), which have distinct mutagenic properties. As UVC is absorbed by the ozone layer, not reaching Earth's surface, skin is daily exposed to UVB and UVA (1). During past decades, UVB was considered to be more genotoxic than UVA (2). Due to their strong absorption by DNA, UVB generates photoproducts, that is cyclobutane pyrimidine dimers (CPDs), pyrimidine (6-4) pyrimidone photoproducts (6-4PP), and Dewar isomers, leading to DNA mutations and cancers (3). Once thought to be relatively innocuous, UVA is now known to damage DNA, proteins, and lipids, which can result in harmful consequences, such as carcinogenesis and skin aging. Since 2009, UVA is recognized as a class I carcinogen (4) even if its contribution to sunlight mutagenesis is still unclear. UVA dramatically induces oxidatively induced DNA lesions (5) and leads to bipyrimidine photoproducts as well (6). It has been shown that UVA could also oxidize several DNA repair proteins, which could compromise their activation and efficiency (7). UVA is more than 20 times abundant in sun radiation than UVB and can penetrate the skin deeper (8). Therefore, UVA is very likely to induce genetic damage and mutations in the epidermal basal layer, which hosts of proliferative cells.

Cells protect themselves against genotoxic UV through several endogenous systems, such as melanin (9), antioxidant defenses (10), and DNA repair mechanisms (11). The exogenous use of phytochemicals (*i.e.* dietary antioxidants) as systemic photoprotective agents can contribute to endogenous photoprotection (12,13). This approach, also called photochemoprotection, has found its place in skin care products with the use of plant extracts having photoprotective properties against UV insults (14,15). Such plant extracts are composed of phytochemicals acting as UV absorbers/scatters (16) and/or antioxidants (17) and/or DNA genoprotectors (18,19) upon UVB exposure. Overall, these are antioxidant activities coupled with the improvement of DNA repair capacities that characterize the genoprotective effects of such UVB photoprotective agents. In contrast, there are few studies describing plant extracts able to reduce UVA-induced genotoxic effects in keratinocytes (20–22).

Sechium edule, also known as chayote, is an edible plant belonging to the Cucurbitaceae family used as a laxative in traditional folk medicine. Extracts of *S. edule* fruit also exhibit many biological activities such as preventive and therapeutic efficacies against oxidative stress (23), due to its potent antioxidant properties for inhibiting lipid peroxidation (24). The fruits are rich in amino acids, sugars, saponins, and flavonoids (25). Multiple studies have demonstrated the capacity of several plant polyphenolic compounds, that is flavonoids, to protect epidermis against UV-induced damage (26). Flavonoids are endowed with strong photoprotective activities for fighting oxidative and inflammatory deleterious effects of UV.

*Corresponding author email: nbechetoille@gattefosse.com (Nicolas Bechetoille)

Based on these data, in the current study, we investigated the effect of supplementing primary human keratinocytes with *S. edule* fruit extract (SEE) on UVA protection. We showed that SEE reduced UVA-induced DNA damage with concomitant increase in DNA repair capacities and the maintenance of proliferative capacity of keratinocytes, suggesting a potential cytoprotective and genopreventive effects.

MATERIALS AND METHODS

Preparation of SEE. Fresh mature fruits of chayote (*Sechium edule* (Jacq.) Sw.) were harvested from the island of Reunion, sliced, dried (40°C, hot air ventilation), and grinded into powder. 50 g of powdered sample was extracted under stirring at 70°C for 3 h using 950 g of a natural deep eutectic solvent (fructose/glycerin/water 50:25:25 by weight). The vegetal extract was filtered through cellulose acetate membrane filter (two bars, until 0.22 μm pore size membrane). The appearance of SEE was limpid yellow orange colored liquid. In this study, SEE was tested at five concentrations (0.05%, 0.1%, 0.5%, 1%, and 2%).

Human skin samples. Human skin tissue explants were obtained with the informed consent of patients undergoing surgical discard, in accordance with French ethical guidelines and the declaration to the French Research Ministry (DC no 2008162).

Keratinocyte extraction and culture. Normal human keratinocytes (NHK) were obtained from abdomen biopsies of Caucasian female donors (20 and 25 years old). Epidermis was separated from dermis using 10 mg mL^{-1} dispase (Thermo Fisher Scientific, Waltham, MA). Then, NHK were dissociated using trypsin-EDTA 0.05% (Thermo Fisher Scientific) for 12 min at 37°C. NHK were counted in Malassez after trypan blue coloration. NHK were immediately seeded onto feeder layers (human irradiated fibroblasts preseeded at 4000 cells cm^{-2}) and cultured in keratinocyte medium containing DMEM and Ham's F12 at 3:1 ratio (Thermo Fisher Scientific) supplemented with 10% Fetal Calf Serum (Hyclone, Logan, UT), 10 ng mL^{-1} epidermal growth factor/EGF (Sigma, St Quentin Fallavier, France), 24.3 μg mL^{-1} adenine (Sigma), 0.4 μg mL^{-1} hydrocortisone (Upjohn, Serb Laboratories, Paris, France), 0.12 IU mL^{-1} insulin (Lilly France, St Cloud, France), 2.10^{-9} M triiodo-L-thyronine (Sigma), 10^{-9} M cholera toxin (Sigma), and antibiotics. The culture medium was changed three times a week. NHK between passages 2–3 were used in this study.

Exposure of NHK to UVA. NHK (80–90% confluent or individual keratinocyte (for clonogenic assay)) were irradiated in PBS with UVA doses (25, 50, 75, 100, and 150 J cm^{-2}) using UV system UVA 700L (Waldmann). Control sham-irradiated NHK were used as control. In this study, SEE was removed prior UVA exposure.

Pre- and full-treatment of NHK with SEE. In the pretreatment, NHK (80–90% confluent) were incubated for 24 h with SEE diluted at 0.5% in the culture medium. Then, NHK were washed with PBS and harvested for analysis of genes expression and DNA repair chips assay. After the pretreatment with SEE, NHK were also irradiated with UVA (50 J cm^{-2}) while fully submerged in fresh PBS. Immediately after UVA exposure, NHK were harvested for the detection of reactive oxygen species (ROS) and induction of DNA damage (Fpg-sensitive sites and CPD). In the full-treatment, NHK were firstly pretreated with SEE (0.5%) before being irradiated with UVA (50 J cm^{-2}) and then treated with fresh SEE (0.5%) for additional 24 h. NHK were then washed with PBS and immediately harvested for MTT assay, clonogenic assay, and CPD repair. Untreated NHK were used as control.

MTT assay. Cell viability was evaluated using a 3-(4,5-dimethylthiazol-2-yl)-2,5-diphenyltetrazolium bromide (MTT) assay (Sigma). NHK were incubated in MTT solution (0.1 mg mL^{-1}) for 2 h at 37°C. Then, MTT was removed and NHK were incubated in DMSO for 30 min under gentle agitation. The presence of blue formazan was measured at 550 nm using a microplate reader Infinite M1000 (TECAN). Results are expressed as the viability % *vs* control sham-irradiated NHK (as 100% of viable cells).

Clonogenic assay. NHK were detached using trypsin-EDTA 0.5% (Sigma) and immediately seeded at clonal density (60 cells cm^{-2}) onto feeder layer (inactivated human fibroblasts as preseeded at 4000 cell cm^{-2}) in keratinocyte medium. NHK were cultured for 14 days, and medium was changed three times a week. For clones staining, NHK were fixed and colored using rhodamine (Sigma) at 0.01 g mL^{-1} in 4% paraformaldehyde for 30 min. Holoclones, meroclones, and paraclones were counted using stereomicroscope system (Olympus SZX9).

Determination of intracellular ROS content. NHK were incubated for 10 min with CM-H2DCFDA probe (Thermo Fisher Scientific) at 2.5 μM in PBS. Then, NHK were washed with PBS and immediately irradiated with UVA (50 J cm^{-2}). NHK were detached using trypsin-EDTA 0.5% (Sigma) and immediately analyzed by flow cytometry (BD FACSCalibur™) using BD CellQuest Pro software (BD Biosciences, Le Pont de Claix, France). The amount of ROS production was evaluated as the mean fluorescence intensity (MFI).

Quantification of Fpg-sensitive sites by alkaline Comet assay. Cell suspensions containing 2.10^5 NHK/50 μl were mixed with 450 μl of 0.7% prewarmed low-melting-point agarose in PBS. 100 μl of this cell suspension mixture was spread on microscopic slides coated with 1% agarose and then chilled to ice temperature. After gelling, slides were treated with lysis solution pH 10 (2.2 M NaCl, 89 mM Na-EDTA, 8.9 mM Tris buffer, 30 mM *N*-lauroyl sarcosine, 10% DMSO, 1% Triton X-100 [all from Sigma]) overnight at 4°C. Then, the formamidopyrimidine-DNA glycosylase (Fpg, Trevigen, Gaithersburg, MD) was added at 0.05 U μl^{-1} for 45 min at 37°C. The slides were washed with 0.4 M Tris buffer pH 7.4 and submerged in horizontal chamber in electrophoresis buffer (0.3 M NaOH, 1 mM Na-EDTA) for 20 min at 4°C. Electrophoresis was carried out at 300 mA at 4°C for 30 min. The slides were neutralized with Tris buffer (0.4 M, pH 7.4) and stained with 50 μl of GelRed (Biotium, Fremont, CA). The slides are immediately stored at 4°C in a light-tight wet chamber until analysis. Comet analysis was performed using Axioskop 2 Plus microscope (ZEISS) and the image analysis Komet six software (Kinetic Imaging Ltd, Andor Technology plc. Belfast, Ireland). The median % of tail intensity was taken as the index of damage. For each condition, the average % of tail intensity was determined from the analysis of 150 comets (triplicate slides, 50 comets analyzed per slides). Oxidized purines were calculated by subtraction of damage obtained with and without Fpg.

Quantification of CPDs by HPLC/MS-MS. DNA extraction. DNA was extracted as previously described by Genies *et al.* (27). Briefly, NHK were suspended in Triton-containing buffer for lysing cellular membrane and nuclei were collected by centrifugation (1500 ***g***, 5 min). Then, nuclear membrane was lysed in a SDS-containing buffer and RNA was removed by incubation with a RNase mixture (RNase A 100 mg ml^{-1} and T1 1 U μl^{-1}) for 15 min at 50°C. Proteins were hydrolyzed by incubation for 1 h at 37°C after addition of protease (20 mg ml^{-1}). DNA was precipitated by addition of a concentrated NaI solution and of absolute isopropanol. After rinsing with ethanol, DNA was suspended in 50 μL of aqueous solution and hydrolyzed in two successive steps. Samples were first incubated for 2 h at 37°C in pH 6 buffer containing phosphodiesterase II (0.005 U), DNase II (0.5 U), and nuclease P1 (0.5 U). Then, pH was adjusted to 8 and a second incubation was performed with phosphodiesterase I (0.05 U) and alkaline phosphatase (2 U). The reaction was stopped with HCl 0.1 N. After centrifugation (5000 ***g***, 5 min.), the DNA hydrolysate was collected, transferred into HPLC vials, lyophilized, and suspended in water for HPLC-tandem mass spectrometry (HPLC-MS/MS) analysis.

Separation and detection. The digested sample was injected into the HPLC system consisting in Agilent series 1100 system equipped with a Uptisphere ODB reverse phase column (2 × 250 mm ID, particle size 5 μm; Interchim, Montluçon, France). The mobile phase was a gradient of acetonitrile in a 2 mM aqueous solution of triethylammonium acetate. A UV detector set at 260 nm was used to quantify normal nucleosides in order to determine the amount of analyzed DNA. The HPLC flow was then directed toward an API 3000 electrospray triple quadrupole mass spectrometer operating in the negative ionization mode. The detection of TT-CPD, TC-CPD, or CT-CPD was performed in the "multiple reaction monitoring" mode. Two fragmentations were monitored: 545 $[M–H]^-$) → 447 [M–dehydrated 2-deoxyribose–$H]^-$) and 545 $[M–H]^-$) → 195 [phosphorylated 2-deoxyribose–$H]^-$). External calibration was achieved for both detectors using authentic compounds.

Expression of OGG1, MYH, XRCC1, APE1, UNG, LIG3, and POLβ genes. RNA extraction and retrotranscription. Total RNA was extracted with the GenElute mammalian total RNA miniprep kit (Sigma). RNA integrity was assessed by verifying the 260/280 nm absorbance ratio between 1.7 and 2.1 and using native gel electrophoresis. An amount of

500 ng per sample in native agarose gel loading buffer (15% Ficoll, 0.25% xylene cyanol, 0.25% bromophenol blue) was loaded on 1% agarose gel in TBE (89 mM Tris-HCl pH 7.8, 89 mM borate, 2 mM EDTA) with 0.5 μg mL^{-1} ethidium bromide (Sigma) added to the gel. The gel was then run at 5–6 V cm^{-1} measured between the electrodes. Total RNA was considered as intact when two sharp 28S and 18S rRNA bands were visualized, with a 2:1 (28S:18S) ratio in term of intensity.

Total RNA was reverse transcribed using Superscript II Reverse Transcriptase™ (Invitrogen) according to the manufacturer's protocol. Briefly, 2 μg of total RNA was heated with 100 ng of Random Hexamers Primers (Promega SARL, Charbonnières, France) and 10 nmol of dNTPs mix (Sigma) for 5 min at 70°C and quick chilled on ice. Then, first-strand buffer to a final concentration of 1×, 0.1 M DTT and 45 U of ribonuclease inhibitor (Sigma) were added to the mixture and incubated for 2 min at 25°C. Superscript II Reverse Transcriptase™ (200 U) was finally added to the mixture and incubated first for 10 min at 25°C and next for 50 min at 42°C. The reaction was stopped by heating for 15 min at 70°C.

Real-time quantitative PCR. Gene specific oligonucleotide primers (OGG1: TGG-AAG-AAC-AGG-GCG-GGC-TA (forward), ATG-GAC-ATC-CAC-GGG-CAC-AG (reverse); MYH: CCA-GAG-AGT-GGA-GC A-GGA-AC (forward), TTT-CTG-GGG-AAG-TTG-ACC-AC (reverse); XRCC1: CAG-CCC-TAC-AGC-AAG-GAC-TC (forward), GCT-GTG-ACT-GGG-GAT-GTC-TT (reverse)) were designed using Primer3-web 0.4.0 (http://primer3.sourceforge.net.sci-hub.cc) and obtained from a commercial supplier (Eurogentec SARL, Angers, France). Quantitative PCR (qPCR) was performed in a MX3005p Multiplex Quantitative PCR system (Stratagene, La Jolla, CA) using MESA Blue qPCR™ Mastermix Plus for SYBR® Assay Low Rox (Eurogentec, Angers, France). qPCRs were carried out in triplicate in 25 μL reaction volumes containing 200 nM forward and reverse primers and 20 ng samples of DNA using the following program: 5 min at 95°C, and 40 cycles of 15 s at 95°C, 20 s at 55°C, and 40 s at 72°C with fluorescence acquisition at the end of the 55°C primer annealing step. The integrity of amplification indicated by a single melt peak for each product was verified by a dissociation curve analysis at 95°C for 1 min, 55°C for 30 s and 95°C for 30 s with fluorescence acquisition at all points from 55 to 95°C. The built in amplification-based proprietary algorithm (Stratagene) was used to set the fluorescence threshold value. This algorithm determined the portion of the amplification plots where all of the data curves displayed an exponential increase in fluorescence, and calculated the threshold value that minimized the standard deviation in C_t values for each replicate set at a point which fell within 32.5% of the fluorescence shift for all the curves. The number of cycles (C_t) at which the amplification-corrected normalized fluorescence (dRn) for each reaction crossed the threshold value was used to interpret results.

Results expression. The mean fold change (FC) was calculated with the following calculation:

$$\mathrm{FC} = 2^{C_t\text{target gene/control} - C_t\text{target gene/SEE}} \times 2^{C_t\mathrm{GAPDH/control} - C_t\mathrm{GAPDH/SEE}}$$

The gene expression was considered as significantly upregulated when FC was superior to 1.2.

DNA repair chips assay. Cell nuclear extracts. Nuclear extracts were prepared as described by Millau *et al.* (28). Briefly, NHK were washed twice in ice-cold PBS, suspended in ice-cold buffer A (10 mM HEPES pH 7.9, 1.5 mM $MgCl_2$, 10 mM KCl, 0.01% Triton X-100, 0.5 mM DTT, and 0.5 mM PMSF), and left on ice for 20 min. Cells were vortexed to achieve complete cytosol membrane lysis. Then, nuclei were recovered by centrifugation (2991 ***g***, 5 min) at 4°C and suspended in ice-cold buffer B (10 mM HEPES pH 7.9, 1.5 mM $MgCl_2$, 400 mM KCl, 0.2 mM EDTA, 25% glycerol, 0.5 mM DTT, antiproteases [Complete-mini, Roche, Meylan, France] and 0.5 mM PMSF). Nuclear membranes were lysed on ice for 20 min, and two cycles of freezing–thawing were performed at −80°C and 4°C, respectively. Finally, the extracts were centrifuged (20217 ***g***, 10 min) at 4°C and the supernatants were recovered. Protein content was determined using the *UPTIMA* BC Assay Protein Quantitation Kit (Interchim, Montluçon, France).

DNA repair chips assay. Slides functionalized by series of lesions-bearing plasmids and lesion-free plasmids (control plasmid) were prepared by LXRepair (Grenoble, France). Three categories of damaged plasmids were used containing the following lesions: photoproducts, that is CPD and 6-4PP, generated by UVC irradiation (CPD-64 plasmid), abasic sites generated by acidic treatment at pH 4.8 (AbaS plasmid), and cytosine and thymine glycols formed by treatment with $KMnO_4$ (glycol plasmid). Each plasmid spot was duplicated, and control plasmids were deposited on each biochip besides to damaged plasmids.

Excision/synthesis repair reaction. The excision/synthesis repair reactions were conducted for 3 h at 30°C. The repair mix (25 μL) containing 5× ATG buffer (200 mM Hepes KOH pH 7.8, 35 mM $MgCl_2$, 2.5 mM DTT, 1.25 mM dATP, 1.25 mM dTTP, 1.25 mM dGTP, 17% glycerol, 50 mM phosphocreatine [all from Sigma]), 10 mM EDTA, 250 g mL^{-1} creatine phosphokinase, 0.5 mg mL^{-1} BSA), 1 mM ATP (Sigma), 1.25 M dCTP-Cy3 (Sigma), and nuclear extracts at the final protein concentration of 0.15 mg mL^{-1} were deposited onto the damaged plasmids after injection into adhesive reaction chambers (Grace Bio-Labs, Oregon). Then, slides were washed in PBS/Tween 0.05%, centrifuged (59 ***g***, 3 min), and dried (30°C, 5 min) in an incubator. All samples were run in duplicate.

Fluorescence quantification and data analysis. Images were acquired by scanning the biochip at 532 nm using the InnoScan710AL scanner (Innopsys, Carbonne, France), and the total spot fluorescence intensity (FI) was quantified using the Mapix software (Innopsys). Data were normalized using NormalizeIt software as described by Millau *et al.* (28). Each sample was characterized by six values corresponding to FI measured in five damaged DNA plasmids and that in the control plasmid. The FI of the control plasmid, corresponding to nonspecific repair, was subtracted to the FI obtained for each damaged DNA plasmid. To determine the effects of SEE on DNA repair activities, we calculated the following ratio: FI (SEE condition)/FI (untreated) for each lesion in all experiments. Ratio >1 meant increased DNA repair activities.

Statistical analysis. Results were expressed as the means ± SD (three independent experiments). Statistical analysis between controls and treatments were performed by Student's *t*-test, where a $P \leq 0.05$ was considered statistically significant.

RESULTS

SEE protects NHK against UVA-induced cytotoxicity

First, to establish a noncytotoxic SEE treatment, we evaluated the effect of five concentrations (0.05%, 0.1%, 0.5%, 1%, and 2%) of SEE preparations on the cell viability of NHK (See Figure S1). For further experimentation, we chose the 0.5% concentration which showed no significant decrease ($P \geq 0.05$) in NHK cell viability as compared to the untreated control. Next, by considering the previous study using the same irradiation unit (29), we assessed a range of UVA doses on the cell viability of NHK. We showed that the more the UVA doses increased, the more the cell viability of NHK decreased (Figure S2). For this study, we selected the 50 J cm^{-2} UVA dose, which was enough to cause an approximate 30% decrease in NHK cell viability.

We showed that cell viability of SEE-treated NHK, UVA irradiated or not, was close to that of control sham-irradiated NHK (Fig. 1). Thus, the UVA-induced cytotoxicity of NHK was fully prevented by the SEE treatment. Therefore, SEE would protect NHK against short-term cytotoxic effects induced by UVA.

SEE maintains clonogenic potential of NHK after exposure to UVA

To evaluate the long-term UVA effects on NHK, we performed clonogenic assays for measuring both maintenance of cell proliferative capacity and preservation of stemness property of cells. We showed that the number of colonies was not decreased in UVA-irradiated NHK, which demonstrate the absence of UVA-induced toxicity at long-term with our dose, while the type of

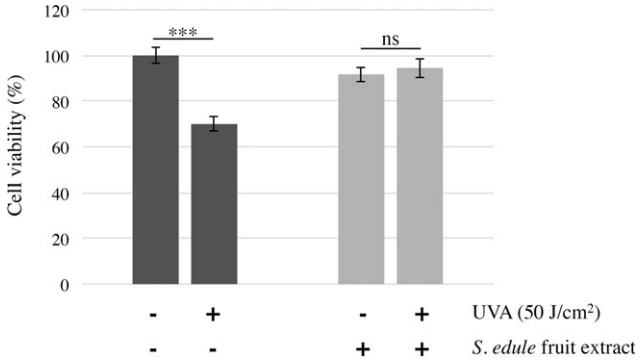

Figure 1. Protective effect of *Sechium edule* fruit extract (SEE) against short-term UVA-induced cytotoxicity in NHK. NHK were pretreated with SEE (0.5%) for 24 h and irradiated (or not) with 50 J cm^{-2} UVA. Then, NHK were post-treated with fresh SEE (0.5%) for additional 24 h. The cell viability was evaluated by MTT assay. SEE treatment fully prevented the UVA-induced cytotoxicity in NHK. Data are expressed as the cell viability % *vs* control sham-irradiated and untreated NHK (as 100% of viable cells). The representative data are shown as mean ± SD from three independent experiments ($n = 3$). Statistical analysis is performed using Student's *t*-test. ***$P < 0.001$; ns: not significant.

colony changed from holoclones into meroclones (Fig. 2). Unexpectedly, the treatment with SEE maintained the presence of larger number of characteristic holoclones in UVA-irradiated NHK. Furthermore, it is to be noticed that treatment with SEE alone had even increased the number of colonies and the holoclones number as well. Thus, SEE would have protective effect on both cell replicative senescence and that induced by UVA irradiation.

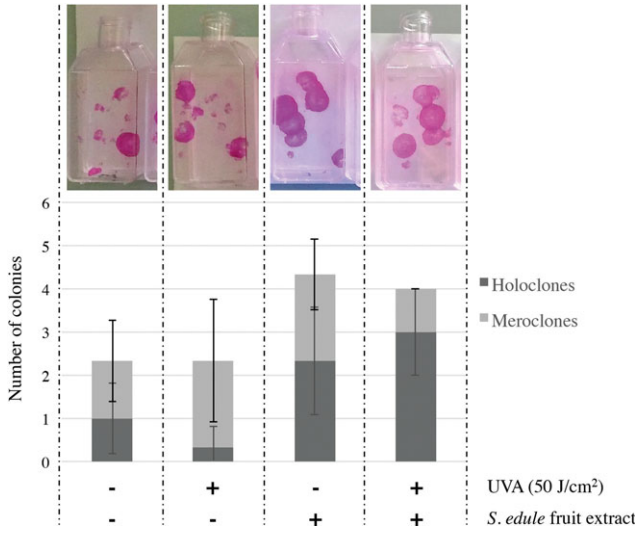

Figure 2. Protective effect of *Sechium edule* fruit extract (SEE) against long-term clonogenic damages induced by UVA in NHK. NHK were pretreated with SEE (0.5%) for 24 h and irradiated (or not) with 50 J cm^{-2} UVA. Then, NHK were post-treated with fresh SEE (0.5%) for additional 24 h. Clonogenic assay was performed by culturing NHK at clonal density (60 cells cm^{-2}) for 14 days. SEE treatment improved the clonogenic potential in control sham-irradiated NHK in addition to fully prevent the loss of such a potential in UVA-irradiated NHK. For the staining of colonies, pictures are representative of three independent experiments ($n = 3$). For the counting of colonies, data are expressed as the number of colonies. The representative data are shown as mean ± SD from three independent experiments ($n = 3$).

SEE decreases UVA-induced oxidative damage in NHK

The main DNA oxidation product of UVA irradiation has been identified in several types of isolated cells (30) and human skin (29) as 8-oxo-7,8-dihydroguanine (8-oxoGua), mainly through the generation of ROS such as singlet molecular oxygen ($^1O_2$) and hydroxyl radical ($^{\cdot}OH$). By FACS analysis, we first analyzed the intracellular levels of ROS by CM-H2DCFDA assay immediately after 50 J cm^{-2} UVA exposure. As expected, we showed that the mean fluorescence intensity of ROS significantly increased in UVA-irradiated NHK compared to control sham-irradiated NHK (Fig. 3). However, SEE treatment significantly decreased the mean fluorescence intensity by 30% ($P < 0.001$) after UVA exposure, meaning that the ROS level in SEE-treated NHK was much lower than that in untreated NHK. Using the comet assay combined with a treatment with bacterial formamidopyrimidine glycosylase, we studied oxidized purines, and in particular 8-oxoGua. Not surprisingly, we showed that UVA irradiation strongly induced Fpg-sensitive sites in NHK (Fig. 4). To a lesser extent, SEE-treated NHK still displayed Fpg-sensitive sites after UVA exposure but with a median percentage of tail intensity lower (−68%, $P < 0.001$) than that of untreated NHK. These results suggested that SEE efficiently reduced both ROS production and oxidative DNA damage induced by UVA.

SEE decreases UVA-induced CPD lesions and stimulates its repair

CPDs are predominant DNA lesions in human skin exposed to UVA irradiation (29). To determine whether SEE could reduce such UVA-induced photoproducts in NHK, we accurately quantified the number of CPD in UVA-irradiated NHK using HPLC/MS-MS. We showed that no CPDs were detected in both control sham-irradiated NHK and SEE-treated NHK (Fig. 5a). Furthermore, the amount of CPD largely increased and immediately following UVA exposure. Even at 24 h post-UVA irradiation, there were still about 60% of remaining CPD in untreated NHK (Fig. 5b). With SEE treatment, the number of CPD in NHK was

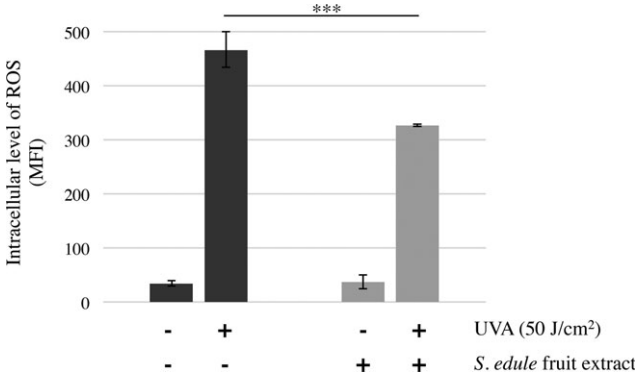

Figure 3. *Sechium edule* fruit extract (SEE) treatment decreases reactive oxygen species (ROS) production in NHK after UVA irradiation. NHK were pretreated with SEE (0.5%) for 24 h and irradiated (or not) with 50 J/cm^2 UVA. The intracellular ROS content was quantified using CM-H2DCFDA probe and FACS analysis. SEE treatment significantly decreased the ROS production in UVA-irradiated NHK. Data are expressed as mean fluorescence intensity (MFI). The representative data are shown as mean ± SD from three independent experiments ($n = 3$). Statistical analysis is performed using Student's *t*-test. ***$P < 0.001$.

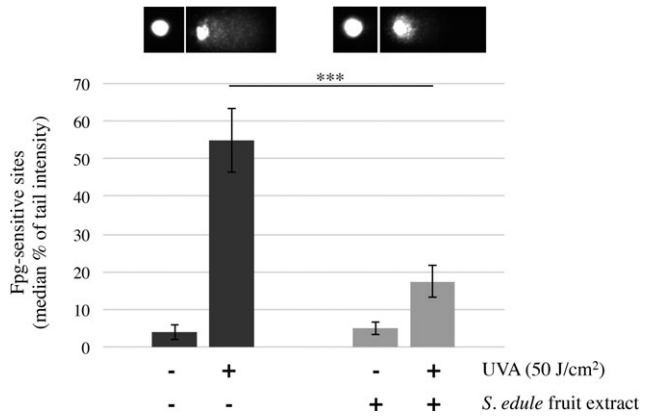

Figure 4. *Sechium edule* fruit extract (SEE) treatment decreases induction of Fpg-sensitive sites in NHK after UVA exposure. NHK were pretreated with SEE (0.5%) for 24 h and irradiated (or not) with 50 J cm^{-2} UVA. The quantification of Fpg-sensitive sites was performed by alkaline Comet assay with FPG digestion. SEE treatment significantly decreased the formation of Fpg-sensitive sites in UVA-irradiated NHK. Pictures are representative of three independent experiments ($n = 3$). Data are expressed as median % of tail intensity. The representative data are shown as mean ± SD from three independent experiments ($n = 3$). Statistical analysis is performed using Student's *t*-test. ***$P < 0.001$.

decreased by 10% ($P < 0.001$) immediately after UVA. At 24 h post-UVA irradiation, the number of remaining CPD was still lower (−32%, $P < 0.001$) in SEE-treated NHK than untreated NHK. These results suggested that SEE effectively reduced the CPD damage in addition to stimulate the repair of such photoproducts.

SEE improves global DNA repair capacities in NHK

Oxidative DNA bases modified by ROS, primarily as 8-oxoGua, are repaired through the base excision repair (BER) pathway. A set of key genes, involved in BER system, was therefore investigated in SEE-treated NHK. Although the expression levels of *XRCC1*, *APE1*, *UNG*, *LIG3,* and *POLβ* genes were unchanged (data not shown), we showed that mRNA levels of *OGG1* and *MYH* were upregulated by 5.63-fold ($P < 0.001$) and 1.86-fold ($P < 0.01$), respectively, in SEE-treated NHK (Fig. 6). To go further, we also evaluated the enzymatic repair activities of several DNA lesions involving both BER and nucleotide excision repair (NER). Using repair plasmid biochips, we showed that the SEE treatment significantly increased the enzymatic repair activities toward abasic sites (1.44-fold, $P < 0.01$), CPD-64 (2.30-fold, $P < 0.001$), and thymine glycols (1.66-fold, $P < 0.01$) in NHK (Fig. 7). Thus, SEE would improve global DNA repair pathways for better repairing small oxidative lesions and photoproducts in NHK.

DISCUSSION

The skin is the largest organ of the body and the most exposed to UV irradiation. The past decade has seen a surge in the incidence of skin cancer due to changes in life style patterns (*i.e.* tanned skin trend) that have led to a significant increase in the amount of UV irradiation that people receive. Therefore, in the recent years, the research for new products with protective effect in the skin cells has been carried out to prevent deleterious effects of UV. In this context, our present study demonstrated the photoprotective effects of SEE to fight against UVA-induced DNA damage in normal human keratinocytes.

Thanks to their antioxidant, anti-inflammatory, antimutagenic, anticarcinogenic, and immunomodulatory properties, natural agents can exert striking inhibitory effects on cellular and molecular events and, therefore, are gaining considerable attention for the prevention of UV-induced damage. The use of plants, herbs, or spices is an add on the existing strategies for fighting against damage from excessive exposure to UV. Indeed, several natural agents (*i.e.* tea polyphenols, pomegranate, delphinidin, cyaniding, resveratrol, genistein, silymarin, quercetin, luteolin, kaempferol, lycopene, sulforaphane, honokiol, caffeine, grape seed proanthocyanidins) have the ability to inhibit or reduce the adverse biological effects of UVB (31). In contrast, there are very few plant extracts, that is *Vaccinium myrtillus* (20), *Prunella vulgaris* (21), and *Thymus vulgaris* (22), which are described for preventing harmful damage induced by UVA. Moreover, these studies lack the molecular mechanisms underlying the photochemoprotection activity of such compounds. In this study, we introduced a fruit

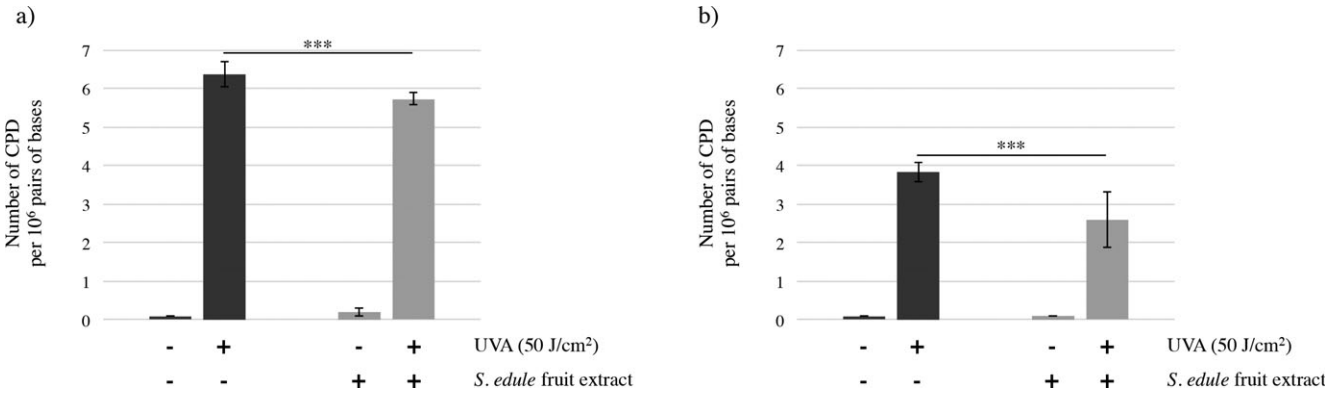

Figure 5. Protective effect of *Sechium edule* fruit extract (SEE) against UVA-induced CPD damage in NHK. NHK were pretreated with SEE (0.5%) for 24 h and irradiated (or not) with 50 J cm^{-2} UVA. After UVA exposure, either NHK were immediately analyzed for CPD quantification (a) or NHK were post-treated with fresh SEE (0.5%) for additional 24 h and then analyzed for CPD quantification (b). The CPD quantification was performed by HPLC/MS-MS. SEE treatment significantly decreased the number of CPD in addition to speed up their repair in UVA-irradiated NHK. Data are expressed as the number of CPD per 106 pairs of bases. The representative data are shown as mean ± SD from three independent experiments ($n = 3$). Statistical analysis is performed using Student's *t*-test. ***$P < 0.001$.

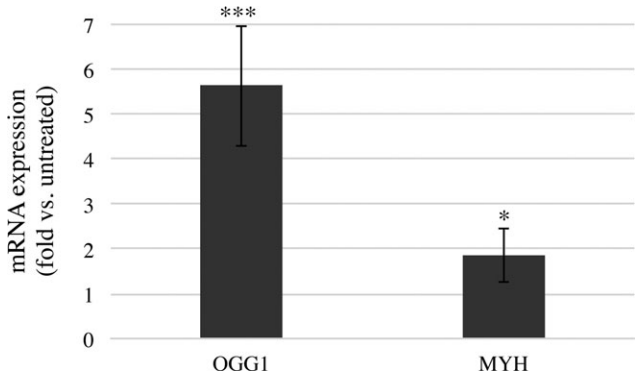

Figure 6. *Sechium edule* fruit extract (SEE) increases mRNA expression of *OGG1* and *MYH* in NHK. NHK were treated with SEE (0.5%) for 24 h. Then, mRNA expression of targeted genes was quantified by real-time quantitative PCR. SEE treatment significantly increased the mRNA expression of both *OGG1* and *MYH* in NHK. Data are expressed as the mean fold change *vs* untreated NHK. The representative data are shown as mean ± SD from three independent experiments ($n = 3$). Statistical analysis (*vs* untreated control) is performed using Student's *t*-test. ***$P < 0.001$; *$P < 0.05$.

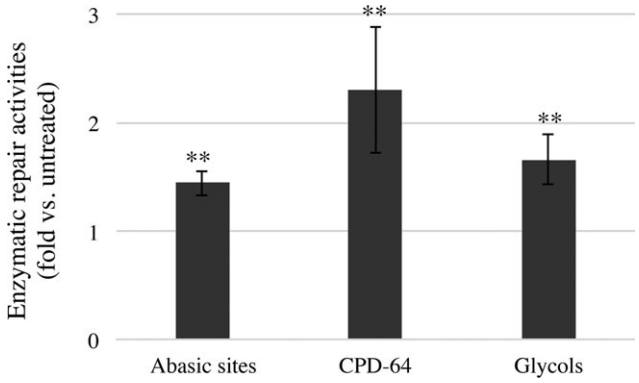

Figure 7. *Sechium edule* fruit extract (SEE) increases enzymatic repair activities in NHK. NHK were treated with SEE (0.5%) for 24 h. Then, a DNA repair chips assay was performed to evaluate enzymatic repair activities of abasic sites, CPD-64 and glycols. SEE treatment significantly increased the enzymatic repair activities of the three DNA lesions in NHK. Data are expressed as the fold of fluorescence intensity *vs* untreated NHK. The representative data are shown as mean ± SD from three independent experiments ($n = 3$). Statistical analysis (*vs* untreated control) is performed using Student's *t*-test. **$P < 0.01$.

extract of *S. edule* as a novel botanical agent in chemoprevention of UVA-induced carcinogenesis and photoaging.

UVA exerts their deleterious biological effects, among others, by the generation of ROS. Overproduction of ROS results in oxidative stress damaging lipids, proteins and DNA. The pre-treatment of normal human keratinocytes with SEE decreased by 30% the intracellular content of ROS after UVA exposure, suggesting that SEE could be useful in attenuation of UVA-induced oxidative stress. Because SEE was totally removed during UVA irradiation, we can exclude a physical filter effect. The skin cells are rich in ROS detoxifying enzymes, such as superoxide dismutase, glutathione peroxidase, glutathione, and catalase, for maintaining the redox balance termed also redox homeostasis. Under UVA irradiation, the cutaneous enzymatic antioxidant system, and more particularly catalase, was depleted (32) leading to a disturbance of balance between ROS production and antioxidant defenses. In the present study, SEE would seem to protect this redox homeostasis by limiting the ROS production. Moreover, SEE could act as a ROS quencher because the *S. edule* plant contains flavonoids as antioxidant molecules (25). However, more studies still need to be carried out to clarify the photoprotective mechanisms of SEE, such as its properties on the antioxidant enzyme activities and its effects in terms of lipid peroxidation and protein oxidation.

UVA irradiation induces both direct (CPDs) and indirect (oxidative DNA damage) DNA lesions. The main DNA oxidation product is 8-oxoGua that is mostly produced by $^1O_2$ with a small contribution of $^{\cdot}OH$ (33). Our results clearly showed that treatment with SEE affords significant protection against Fpg-sensitive sites (8-oxoGua), which may be partly due to decreased ROS production or increased oxidative DNA repair capacity. The formation of CPD is the predominating type of UVA-mediated damage in both cells and human skin (34–36), and it is on average five times higher than that of 8-oxoGua (30,37). We also confirmed that SEE is able to reduce the number of CPD lesion in UVA-irradiated keratinocytes. Moreover, we showed that SEE treatment also accelerated the CPD repair after 24 h. The mechanism of action by which SEE protects keratinocytes from UVA-induced DNA damage may be partly due to DNA repair capacity strengthened by SEE. In line with these results, we found that the excision/synthesis repair activities for CPD lesions were significantly stronger in SEE-treated keratinocytes. DNA repair, more particularly NER in skin cells, might be compromised under conditions of oxidative stress induced by UVA (38). Indeed, oxidative protein damage severely limits the efficacy of DNA repair proteome (39). By limiting the ROS production, SEE could protect the DNA repair enzymes against oxidation and therefore maintain the DNA repair proteins maximally effective.

The most oxidant-induced base lesions are corrected by the BER system, which involves DNA glycosylases such as 8-oxoguanine DNA glycosylase 1 (OGG1) and MutY-homolog (MYH) (40). OGG1 and MYH which recognize precisely 8-oxoGua are key glycosylases for repairing such oxidative damage (41) and their DNA repair activities are susceptible to inhibition by oxidation (39,42). In this context, we also showed that the SEE treatment increased the mRNA expression of OGG1 and MYH, suggesting that SEE-treated keratinocytes would have a better ability to repair oxidative DNA lesions such as 8-oxoGua, at least at the first step of recognition and excision of lesion. Also, using DNA repair biochips, we showed that SEE-treated keratinocytes have a better excision capacity of thymine glycol which is one of the major toxic oxidative DNA lesions generated by ROS (43) and possesses strong blocking properties for replication and transcription that leads to cell death (44). In the same way, the antioxidant properties of SEE could participate to the preservation of DNA repair by protecting BER system (*i.e.* glycosylases activity), which is compromised under UVA (45), and neutralizing ROS, which oxidize DNA repair proteins. Because OGG1 is inactivated upon UVB exposure (46), there is an interest to protect and/or increase its expression for maintaining the DNA repair and therefore for removal of oxidative damage. The topical application of enzymes, such as OGG1 (47) or T4 endonuclease V (48) for stimulating DNA repair systems can also protect the skin against UV irradiation. As nicotinamide (49), SEE can reduce Fpg-sensitive sites (8-oxoGua) and CPD

by enhancing DNA repair, supporting SEE's potential as an inexpensive, convenient, and nontoxic agent for skin chemoprevention.

The protection of DNA is essential to preserve both stability and integrity of genome. The fate of proliferative keratinocytes can be disrupted by daily UVA doses (from 15 to 20 J cm^{-2} per hour in summer) that induce about 1.4 photoproducts/10^6 bases and 0.1 8-oxoGua/10^6 bases (29). Besides, the cell oxidative metabolism adds to UV-induced deleterious effects to damaged DNA. In our study, we showed that UVA-irradiated keratinocytes exhibiting damaged DNA lost their capacity to produce holoclones. Conversely, SEE-treated keratinocytes exhibiting much less damaged DNA and kept their holoclonogenic capacities. Therefore, it is legitimate to make a link between DNA damage in UVA-irradiated keratinocytes and the loss of stemness after UVA exposure. In addition, we can assume a long-term genoprotective effect of SEE in keratinocytes for maintaining the skin homeostasis after UVA exposure. It is also noteworthy that SEE could preserve the stemness of keratinocytes during replicative senescence.

The tests performed in this study do not allow us to fully understand the mechanisms of action by which SEE protects keratinocytes from UVA irradiation. As it has been reported that ROS can act as signal transduction molecules that induce proinflammatory cytokines and the NF-kB pathway (50), it will be interesting to investigate the anti-inflammatory properties of SEE and more particularly its effects on the mitogen-activated protein kinases (MAPK) cascade. Because of UV-induced DNA damage being one of the earliest molecular events in the development of immune suppression, the SEE would be able to prevent UV-induced immunosuppression through rapid repair of UV-induced DNA damage in the form of CPD. The chemical composition of our SEE is currently ongoing, and the exact identification of the components that are responsible for the biological activities will have to be known.

In conclusion, our data demonstrate that SEE treatment effectively protected keratinocytes from long-term adverse effects of UVA by decreasing the oxidative stress at cellular and DNA levels and increasing DNA repair mechanisms. Thus, the application of SEE may exert photochemopreventive effects against skin cancer and photoaging.

Acknowledgements—We are grateful to Thierry Douki, Camille Cuier, Sylvain Caillat, David Beal, and Véronique Collin-Faure for their technical assistance for mass spectrometry and flow cytometry. We are grateful to Nour Fayyad for reading and correcting the manuscript.

This work was supported by the Gattefossé company (Saint-Priest, France) specialized in lipid chemistry and plant extraction for Health and Beauty industries. Elodie Metral was supported by a grant from Gattefossé.

SUPPORTING INFORMATION

Additional Supporting Information may be found in the online version of this article:

Figure S1. Assessment of NHK cell viability after SEE treatment.

Figure S2. Assessment of NHK cell viability after UVA irradiation.

REFERENCES

1. Schuch, A. P., C. C. M. Garcia, K. Makita and C. F. M. Menck (2013) DNA damage as a biological sensor for environmental sunlight. *Photochem. Photobiol. Sci.* **12**, 1259–1272.
2. de Gruijl, F. R. (2002) Photocarcinogenesis: UVA vs. UVB radiation. *Skin Pharmacol. Appl. Skin Physiol.* **15**, 316–320.
3. Lucas, R. M., M. Norval, R. E. Neale, A. R. Young, F. R. de Gruijl, Y. Takizawa and J. C. van der Leun (2015) The consequences for human health of stratospheric ozone depletion in association with other environmental factors. *Photochem. Photobiol. Sci.* **14**, 53–87.
4. El Ghissassi, F., R. Baan, K. Straif, Y. Grosse, B. Secretan, V. Bouvard, L. Benbrahim-Tallaa, N. Guha, C. Freeman, L. Galichet and V. Cogliano (2009) A review of human carcinogens–part D: Radiation. *Lancet Oncol.* **10**, 751–752.
5. Cadet, J., T. Douki and J.-L. Ravanat (2015) Oxidatively generated damage to cellular DNA by UVB and UVA radiation. *Photochem. Photobiol.* **91**, 140–155.
6. Douki, T., A. Reynaud-Angelin, J. Cadet and E. Sage (2003) Bipyrimidine photoproducts rather than oxidative lesions are the main type of DNA damage involved in the genotoxic effect of solar UVA radiation. *Biochemistry* **42**, 9221–9226.
7. Brem, R., M. Guven and P. Karran (2017) Oxidatively-generated damage to DNA and proteins mediated by photosensitized UVA. *Free Radic. Biol. Med.* **107**, 101–109.
8. Lim, H.W., M. Naylor, H. Honigsmann, B.A. Gilchrest, K. Cooper, W. Morison, V.A. Deleo and L. Scherschun (2001) American Academy of Dermatology Consensus Conference on UVA protection of sunscreens: Summary and recommendations. Washington, DC, Feb 4, 2000. *J. Am. Acad. Dermatol.* **44**, 505–508.
9. Kobayashi, N., A. Nakagawa, T. Muramatsu, Y. Yamashina, T. Shirai, M. W. Hashimoto, Y. Ishigaki, T. Ohnishi and T. Mori (1998) Supranuclear melanin caps reduce ultraviolet induced DNA photoproducts in human epidermis. *J. Invest. Dermatol.* **110**, 806–810.
10. Halliwell, B. (1999) Antioxidant defence mechanisms: From the beginning to the end (of the beginning). *Free Radical Res.* **31**, 261–272.
11. Rastogi, R. P., A. Richa, M. B. Tyagi Kumar and R. P. Sinha (2010) Molecular mechanisms of ultraviolet radiation-induced DNA damage and repair. *J. Nucleic Acids* **2010**, 592980.
12. Adhami, V. M., D. N. Syed, N. Khan and F. Afaq (2008) Phytochemicals for prevention of solar ultraviolet radiation-induced damages. *Photochem. Photobiol.* **84**, 489–500.
13. Fernandez-Garcia, E. (2014) Skin protection against UV light by dietary antioxidants. *Food Funct.* **5**, 1994–2003.
14. Afaq, F. and H. Mukhtar (2006) Botanical antioxidants in the prevention of photocarcinogenesis and photoaging. *Exp. Dermatol.* **15**, 678–684.
15. Gonzalez, S., Y. Gilaberte, N. Philips and A. Juarranz (2011) Fernblock, a nutriceutical with photoprotective properties and potential preventive agent for skin photoaging and photoinduced skin cancers. *Int. J. Mol. Sci.* **12**, 8466–8475.
16. Bulla, M. K., L. Hernandes, M. L. Baesso, A. C. Nogueira, A. C. Bento, B. B. Bortoluzzi, L. Z. Serra and D. A. G. Cortez (2015) Evaluation of photoprotective potential and percutaneous penetration by photoacoustic spectroscopy of the Schinus terebinthifolius raddi extract. *Photochem. Photobiol.* **91**, 558–566.
17. Khan, N., D. N. Syed, H. C. Pal, H. Mukhtar and F. Afaq (2012) Pomegranate fruit extract inhibits UVB-induced inflammation and proliferation by modulating NF-kappaB and MAPK signaling pathways in mouse skin. *Photochem. Photobiol.* **88**, 1126–1134.
18. Chen, N., R. Scarpa, L. Zhang, M. Seiberg and C. B. Lin (2008) Nondenatured soy extracts reduce UVB-induced skin damage via multiple mechanisms. *Photochem. Photobiol.* **84**, 1551–1559.
19. Calvo-Castro, L., D. N. Syed, J. C. Chamcheu, F. M. P. Vilela, A. M. Perez, F. Vaillant, M. Rojas and H. Mukhtar (2013) Protective effect of tropical highland blackberry juice (Rubus adenotrichos Schltdl.) against UVB-mediated damage in human epidermal keratinocytes and in a reconstituted skin equivalent model. *Photochem. Photobiol.* **89**, 1199–1207.

20. Calo, R. and L. Marabini (2014) Protective effect of *Vaccinium myrtillus* extract against UVA- and UVB-induced damage in a human keratinocyte cell line (HaCaT cells). *J. Photochem. Photobiol., B* **132**, 27–35.
21. Psotova, J., A. Svobodova, H. Kolarova and D. Walterova (2006) Photoprotective properties of *Prunella vulgaris* and rosmarinic acid on human keratinocytes. *J. Photochem. Photobiol., B* **84**, 167–174.
22. Calo, R., C. M. Visone and L. Marabini (2015) Thymol and Thymus Vulgaris L. activity against UVA- and UVB-induced damage in NCTC 2544 cell line. *Mutat. Res., Genet. Toxicol. Environ. Mutagen.* **791**, 30–37.
23. Tiwari, A. K., I. Anusha, M. Sumangali, D. A. Kumar, K. Madhusudana and S. B. Agawane (2013) Preventive and therapeutic efficacies of *Benincasa hispida* and *Sechium edule* fruit's juice on sweet-beverages induced impaired glucose tolerance and oxidative stress. *Pharmacologia* **4**, 197–207.
24. Firdous, S. M., K. Sravanthi, R. Debnath and K. Neeraja (2012) Protective effect of ethanolic extract and its ethylacetate and n-butanol fractions of *Sechium Edule* fruits against carbon tetrachloride induced hepatic injury in rats. *Int. J. Pharm. Pharm. Sci.* **4**, 354–359.
25. Siciliano, T., N. de Tommasi, I. Morelli and A. Braca (2004) Study of flavonoids of *Sechium edule* (Jacq) Swartz (Cucurbitaceae) different edible organs by liquid chromatography photodiode array mass spectrometry. *J. Agric. Food Chem.* **52**, 6510–6515.
26. Watson, R. R., V. R. Preedy and S. Zibadi (eds.) (2014) *Polyphenols in human health and disease*. Elsevier/Academic Press, Amsterdam, Boston.
27. Genies, C., A. Maitre, E. Lefebvre, A. Jullien, M. Chopard-Lallier and T. Douki (2013) The extreme variety of genotoxic response to benzoapyrene in three different human cell lines from three different organs. *PLoS ONE* **8**, e78356.
28. Millau, J.-F., A.-L. Raffin, S. Caillat, C. Claudet, G. Arras, N. Ugolin, T. Douki, J.-L. Ravanat, J. Breton, T. Oddos, C. Dumontet, A. Sarasin, S. Chevillard, A. Favier and S. Sauvaigo (2008) A microarray to measure repair of damaged plasmids by cell lysates. *Lab Chip* **8**, 1713–1722.
29. Mouret, S., C. Baudouin, M. Charveron, A. Favier, J. Cadet and T. Douki (2006) Cyclobutane pyrimidine dimers are predominant DNA lesions in whole human skin exposed to UVA radiation. *Proc. Natl Acad. Sci. USA* **103**, 13765–13770.
30. Cadet, J., T. Douki, J.-L. Ravanat and P. Di Mascio (2009) Sensitized formation of oxidatively generated damage to cellular DNA by UVA radiation. *Photochem. Photobiol. Sci.* **8**, 903–911.
31. Afaq, F. (2011) Natural agents: Cellular and molecular mechanisms of photoprotection. *Arch. Biochem. Biophys.* **508**, 144–151.
32. Okada, K., Y. Takahashi, K. Ohnishi, O. Ishikawa and Y. Miyachi (1994) Time-dependent effect of chronic UV irradiation on superoxide dismutase and catalase activity in hairless mice skin. *J. Dermatol. Sci.* **8**, 183–186.
33. Cadet, J., T. Douki and J.-L. Ravanat (2008) Oxidatively generated damage to the guanine moiety of DNA: Mechanistic aspects and formation in cells. *Acc. Chem. Res.* **41**, 1075–1083.
34. Cadet, J. and T. Douki (2011) Oxidatively generated damage to DNA by UVA radiation in cells and human skin. *J. Invest. Dermatol.* **131**, 1005–1007.
35. Halliday, G. M. and J. Cadet (2012) It's all about position: The basal layer of human epidermis is particularly susceptible to different types of sunlight-induced DNA damage. *J. Invest. Dermatol.* **132**, 265–267.
36. Cadet, J., S. Mouret, J.-L. Ravanat and T. Douki (2012) Photoinduced damage to cellular DNA: Direct and photosensitized reactions. *Photochem. Photobiol.* **88**, 1048–1065.
37. Courdavault, S., C. Baudouin, S. Sauvaigo, S. Mouret, S. Candeias, M. Charveron, A. Favier, J. Cadet and T. Douki (2004) Unrepaired cyclobutane pyrimidine dimers do not prevent proliferation of UV-B-irradiated cultured human fibroblasts. *Photochem. Photobiol.* **79**, 145–151.
38. McAdam, E., R. Brem and P. Karran (2016) Oxidative stress-induced protein damage inhibits DNA repair and determines mutation risk and therapeutic efficacy. *Mol. Cancer Res.* **14**, 612–622.
39. Gueranger, Q., F. Li, M. Peacock, A. Larnicol-Fery, R. Brem, P. Macpherson, J.-M. Egly and P. Karran (2014) Protein oxidation and DNA repair inhibition by 6-thioguanine and UVA radiation. *J. Invest. Dermatol.* **134**, 1408–1417.
40. Christmann, M., M. T. Tomicic, W. P. Roos and B. Kaina (2003) Mechanisms of human DNA repair: An update. *Toxicology* **193**, 3–34.
41. Boiteux, S., F. Coste and B. Castaing (2016) Repair of 8-oxo-7,8-dihydroguanine in prokaryotic and eukaryotic cells: Properties and biological roles of the Fpg and OGG1 DNA N-glycosylases. *Free Radic. Biol. Med.* **107**, 179–201.
42. Bravard, A., M. Vacher, E. Moritz, L. Vaslin, J. Hall, B. Epe and J. P. Radicella (2009) Oxidation status of human OGG1-S326C polymorphic variant determines cellular DNA repair capacity. *Can. Res.* **69**, 3642–3649.
43. Takao, M., S.-I. Kanno, T. Shiromoto, R. Hasegawa, H. Ide, S. Ikeda, A. H. Sarker, S. Seki, J. Z. Xing, X. C. Le, M. Weinfeld, K. Kobayashi, J.-I. Miyazaki, M. Muijtjens, J. H. J. Hoeijmakers, G. van der Horst and A. Yasui (2002) Novel nuclear and mitochondrial glycosylases revealed by disruption of the mouse Nth1 gene encoding an endonuclease III homolog for repair of thymine glycols. *EMBO J.* **21**, 3486–3493.
44. Trzeciak, A. R., S. G. Nyaga, P. Jaruga, A. Lohani, M. Dizdaroglu and M. K. Evans (2004) Cellular repair of oxidatively induced DNA base lesions is defective in prostate cancer cell lines, PC-3 and DU-145. *Carcinogenesis* **25**, 1359–1370.
45. Eiberger, W., B. Volkmer, R. Amouroux, C. Dhérin, J. P. Radicella and B. Epe (2008) Oxidative stress impairs the repair of oxidative DNA base modifications in human skin fibroblasts and melanoma cells. *DNA Repair* **7**, 912–921.
46. van der Kemp, P., J. C. Auffret, M. Blais, S. Boiteux Bazin and R. Santus (2002) Ultraviolet-B-induced inactivation of human OGG1, the repair enzyme for removal of 8-oxoguanine in DNA. *Photochem. Photobiol.* **76**, 640–648.
47. Wulff, B. C., J. S. Schick, J. M. Thomas-Ahner, D. F. Kusewitt, D. B. Yarosh and T. M. Oberyszyn (2008) Topical treatment with OGG1 enzyme affects UVB-induced skin carcinogenesis. *Photochem. Photobiol.* **84**, 317–321.
48. Yarosh, D., J. Klein, A. O'Connor, J. Hawk, E. Rafal and P. Wolf (2001) Effect of topically applied T4 endonuclease V in liposomes on skin cancer in xeroderma pigmentosum: A randomised study. Xeroderma Pigmentosum Study Group. *Lancet* **357**, 926–929.
49. Surjana, D., G. M. Halliday and D. L. Damian (2013) Nicotinamide enhances repair of ultraviolet radiation-induced DNA damage in human keratinocytes and *ex vivo* skin. *Carcinogenesis* **34**, 1144–1149.
50. Gorrini, C., I. S. Harris and T. W. Mak (2013) Modulation of oxidative stress as an anticancer strategy. *Nat. Rev. Drug Discovery* **12**, 931–947.